A cell-penetrating peptide derived from human lactoferrin with conformation-dependent uptake efficiency.

Falk Duchardt, Ivo R. Ruttekolk, Wouter P. R. Verdurmen, Hugues
Lortat-Jacob, Jochen Bürck, Hansjörg Hufnagel, Rainer Fischer, Maaike van
den Heuvel, Dennis W. P. M. Löwik, Geerten W. Vuister, et al.

A Cell-penetrating Peptide Derived from Human Lactoferrin with Conformation-dependent Uptake Efficiency

Falk Duchardt[‡1,2], **Ivo R. Ruttekolk**[§1], **Wouter P. R. Verdurmen**[§], **Hugues Lortat-Jacob**[¶], **Jochen Bürck**[‖],
Hansjörg Hufnagel[‡], **Rainer Fischer**[‡], **Maaike van den Heuvel**[**], **Dennis W. P. M. Löwik**[**], **Geerten W. Vuister**[‡‡],
Anne Ulrich[‖], **Michel de Waard**[§§3], **and Roland Brock**[‡§4]

From the [‡]Interfaculty Institute for Cell Biology, University of Tübingen, Auf der Morgenstelle 15, 72076 Tübingen, Germany,
the [§]Department of Biochemistry, Nijmegen Centre for Molecular Life Sciences, Radboud University Nijmegen Medical Centre,
6525 GA Nijmegen, The Netherlands, the [¶]Institut de Biologie Structurale, UMR 5075 CEA-CNRS, Université Joseph Fourier,
41 rue Jules Horowitz, 38027 Grenoble Cedex 1, France, the [‖]Karlsruhe Institute of Technology, Forschungszentrum Karlsruhe, IBG-2,
76131 Karlsruhe, Germany, the Departments of [**]Bio-Organic Chemistry and [‡‡]Protein Biophysics, Institute for Molecules and
Materials, Radboud University Nijmegen, Heyendaalseweg 135, 6525 AJ Nijmegen, The Netherlands, and [§§]INSERM U836,
Université Joseph Fourier, Grenoble Neuroscience Institute, Group 3, 38027 Grenoble Cedex 1, France

The molecular events that contribute to the cellular uptake of cell-penetrating peptides (CPP) are still a matter of intense research. Here, we report on the identification and characterization of a 22-amino acid CPP derived from the human milk protein, lactoferrin. The peptide exhibits a conformation-dependent uptake efficiency that is correlated with efficient binding to heparan sulfate and lipid-induced conformational changes. The peptide contains a disulfide bridge formed by terminal cysteine residues. At concentrations exceeding 10 μM, this peptide undergoes the same rapid entry into the cytoplasm that was described previously for the arginine-rich CPPs nona-arginine and Tat. Cytoplasmic entry strictly depends on the presence of the disulfide bridge. To better understand this conformation dependence, NMR spectroscopy was performed for the free peptide, and CD measurements were performed for free and lipid-bound peptide. In solution, the peptides showed only slight differences in secondary structure, with a predominantly disordered structure both in the presence and absence of the disulfide bridge. In contrast, in complex with large unilamellar vesicles, the conformation of the oxidized and reduced forms of the peptide clearly differed. Moreover, surface plasmon resonance experiments showed that the oxidized form binds to heparan sulfate with a considerably higher affinity than the reduced form. Consistently, membrane binding and cellular uptake of the peptide were reduced when heparan sulfate chains were removed.

Cell-penetrating peptides (CPPs)[5] such as antennapedia-derived penetratin (1) and the Tat peptide (2) are widely used tools for the delivery of peptides, proteins, and oligonucleotides into cells (3). Areas of application range from cell biology (4) to biomedical research (5). Most CPPs used to date are of nonhuman origin, but the immunological relevance of these molecules is particularly important to biomedical research. Especially when conjugated to proteins and nanoparticles, these molecules may give rise to an adaptive immune response. Therefore, CPPs such as the human calcitonin-derived peptide (6) and peptides corresponding to signal sequences of human proteins (7) are considered highly attractive import vehicles.

Human lactoferrin (hLF) is an 80-kDa iron-binding glycoprotein of 703 amino acids (8). It constitutes about 15% of human milk protein and also can be found in low concentrations in blood plasma, tears, nasal fluids, saliva, pancreatic, gastrointestinal, and reproductive tissue secretions (9). With antifungal, antimicrobial, and antiviral activities, the protein plays an important role in the innate immune defense (10). In addition to iron depletion (11), the protein exerts its activity through direct interaction with bacterial components (12).

The hLF N-terminal domain in particular carries potent activity against pathogens (13). In the gastrointestinal tract this domain can be cleaved through pepsin digestion resulting in the release of an antimicrobial peptide called lactoferricin (14). Human lactoferricin comprises 49 amino acids (20–68 of the parent sequence) that form a loop stabilized by two disulfide bonds. The peptide contains sections of hydrophobic and positively charged amino acids comparable with those found in numerous peptides that display antimicrobial activity.

It has been demonstrated that antimicrobial peptides and CPPs possess concordant functional characteristics. On one hand, antimicrobial peptides are taken up into mammalian cells (15), and on the other hand CPPs show antimicrobial activity (16). Therefore, we considered whether a lactoferricin-derived

peptide would also have the ability to act as a CPP by entering into mammalian cells.

Here, we report the characterization of a new cell-penetrating peptide derived from the N-terminal domain of human lactoferrin, which corresponds to amino acid residues 38–59 (19–40 of human lactoferricin). The peptide overlaps with the lipopolysaccharide-binding region of lactoferricin (17). The peptide, which shows a well defined structure-activity relationship, enters cells efficiently. The uptake mechanism of the peptide is concentration-dependent. Above a concentration threshold, rapid delivery into the cytoplasm and nucleus is observed, which has been described previously for the arginine-rich CPPs nona-arginine and Tat-derived peptide (18–20). Quite remarkably, the hLF-derived peptide (hereafter, hLF peptide) contains only four arginine and two lysine residues. Instead, an intramolecular disulfide bridge is required for efficient uptake, demonstrating that having a high number of arginine residues in the peptide sequence is not a prerequisite for triggering the rapid import. Instead, for the hLF peptide efficient import is strictly conformation-dependent.

A combination of surface plasmon resonance (SPR), NMR, and circular dichroism experiments revealed conformation-dependent interactions with heparan sulfate proteoglycans and demonstrated that only the cyclic form of the peptide undergoes a conformational transition when interacting with large unilamellar vesicles. Heparinase treatment of cells reduced membrane binding and uptake of the peptide, demonstrating the relevance of heparan sulfate binding for the function of the peptide as a CPP. By using a biotinylated analog of the peptide, we validated the capacity of the peptide to mediate cellular import of a protein cargo. These results illustrate that the hLF peptide is a promising new candidate for a human CPP with a structure-activity relationship that should stimulate further research on the molecular principles that govern CPP interaction with cell membranes.

EXPERIMENTAL PROCEDURES

Cells and Reagents—The human cervical carcinoma cell line HeLa and the rat IEC-6 cell line were obtained from the American Type Culture Collection (Manassas, VA). 1,4-Dithiothreitol was from Merck (Darmstadt, Germany). 3-(4,5-Dimethylthiazol-2-yl)-2,5-diphenyltetrazolium bromide (MTT), heparinases I–III, BSA, and glucose were obtained from Sigma. Rottlerin was from Calbiochem. The Zenon mouse IgG1 Alexa Fluor 647 labeling kit (specific for the Fc part of IgG1 antibodies) was purchased from Invitrogen. The anti-heparan sulfate (HS) VSV-tagged single chain antibody HS4C3 (21) and the mouse anti-VSV (clone P5D4) antibody were a kind gift from Dr. Toin van Kuppevelt (Dept. of Biochemistry, Radboud University Nijmegen Medical Centre, Nijmegen, The Netherlands). TCEP-HCl was obtained from Thermo Fisher Scientific. The phospholipids DPC (dodecylphosphocholine), DMPC (1,2-dimyristoyl-*sn*-glycero-3-phosphocholine), and DMPG (1,2-dimyristoyl-*sn*-glycero-3-phosphoglycerol) used for vesicle preparation were purchased from Avanti Polar Lipids (Alabaster, AL). Biotin-LC-hydrazide was from Pierce. HBS-P buffer (10 mM HEPES, 150 mM NaCl, 3 mM EDTA, 0.005% surfactant P20, pH 7.4) was from Biacore AB (Uppsala, Sweden).

Peptide Synthesis—Unlabeled hLF peptide was supplied by Thermo Fisher Scientific. The other peptides, purchased from EMC Microcollections (Tübingen, Germany), were labeled fluorescently by N-terminal conjugation of 5(6)-carboxyfluorescein. The purity of all peptides was determined by analytical HPLC. The identity of the peptides was confirmed by matrix-assisted laser desorption ionization time-of-flight (MALDI-TOF) mass spectrometry. Peptides with a purity of less than 90% were purified by preparative HPLC.

Peptide Modification—For intramolecular disulfide bond formation, peptides were oxidized by introducing pure oxygen into the peptide solution followed by incubation at 37 °C for 2 h. For reduction of the disulfide bond, 10 mM dithiothreitol was added, and the peptide solution was then incubated for 2 h at 37 °C. Biotinylated hLF peptides (200 μM) were bound to streptavidin-Alexa Fluor 488 conjugates (50 μM) (Invitrogen) by incubation at 4 °C for 12 h in PBS. For analysis of cellular uptake, the solution was diluted 1:10 with medium.

Flow Cytometry—HeLa cells were incubated with medium containing peptides at the indicated concentrations for 45 min at 37 °C. After incubation, cells were washed with medium, detached by trypsinization for 5 min, suspended in PBS, and measured immediately by flow cytometry (BD FACSCalibur system, BD Biosciences). In each case, the fluorescence of 10,000 viable cells was acquired. Viable cells were gated based on sideward and forward scatter.

Confocal Laser Scanning Microscopy—Confocal laser scanning microscopy was performed on an inverted LSM510 laser scanning microscope (Carl Zeiss, Göttingen, Germany) using a Plan-Apochromat 63×/1.4 N.A. oil differential interference contrast lens and a TCS SP5 confocal laser scanning microscope (Leica Microsystems, Mannheim, Germany) equipped with an HCX Plan-Apochromat 63×/N.A. 1.2 water immersion lens. All peptide uptake measurements were performed with living cells.

Incubation with Inhibitor—Cells were treated with rottlerin (20 μM) for 30 min at 37 °C. Then the medium was removed, and medium containing peptide as well as the inhibitor was added. After a 30-min incubation at 37 °C, cells were washed twice with medium and analyzed by confocal laser scanning microscopy or flow cytometry.

Immunofluorescence—HeLa cells were seeded at a density of 1.5×10^4/well in 8-well chambered coverglasses and cultivated to 75% confluency, after which they were incubated with medium containing 33 mIU/ml heparinases I, 8 mIU/ml heparinase II, and 5 mIU/ml heparinase III for 1 h at 37 °C or left untreated. Then the cells were washed with ice-cold HBS/BSA/glucose (10 mM HEPES, 135 mM NaCl, 5 mM KCl, 1 mM MgCl₂, 1.8 mM CaCl₂, pH 7.4, containing 0.1% (w/v) BSA and 5 mM glucose) and incubated with the anti-HS antibody HS4C3 on ice. After 1.5 h of incubation cells were washed with ice-cold HBS/BSA/glucose. For visualization of bound antibodies, the cells were incubated for 1 h with an anti-VSV antibody (P5D4)/Zenon Alexa Fluor 647 conjugate on ice. The antibody staining was analyzed by confocal laser scanning microscopy.

MTT Assay—HeLa cells were seeded in 96-well microtiter plates (1.5×10^4/well) and cultivated overnight. The next day, cells were incubated with peptides for 6 h or 24 h at 37 °C. Cell

viability was measured using the colorimetric MTT dye. Cells were incubated with MTT at a concentration of 1 mg/ml for 4 h. The formazan product was solubilized with SDS (10% (w/v) in 10 mM HCl). Cell viability was determined by measuring the absorbance of each sample relative to a control not treated with peptide at 570 nm using a microplate reader (SpectraMax 340, Molecular Devices).

Preparation of CD Samples—The hLF peptide was dissolved in phosphate buffer to a concentration of 0.1 mM. Reduction of the disulfide bonds was obtained by adding a 30-fold molar excess of TCEP-HCl with subsequent incubation for 2 h at 37 °C. Oxidation of the hLF peptide was obtained by purging pure oxygen for 15 min and subsequent incubation for 2 h at 37 °C. The DMPC and DMPG lipids were dissolved in 50% chloroform, 50% methanol (v/v) to prepare lipid stock solutions. Aliquots of these stock solutions were mixed to obtain the DMPC:DMPG mixture (molar ratio 3:1). Subsequently, the organic solvents were removed under a gentle stream of nitrogen followed by overnight vacuum evaporation to remove the residual solvent from the respective DMPC or DMPC/DMPG lipid films that had been formed in the vial. The lipid layers were dispersed by the addition of phosphate buffer, vigorous vortexing (10 times, 1 min each), and homogenization by 10 freeze-thaw cycles. Finally, large unilamellar vesicles were prepared by means of 11 extrusion cycles using an Avanti Mini-Extruder equipped with a 100-nm polycarbonate filter. Here, the temperature was maintained above 40 °C by thermostatting the extruder block at 50 °C.

For preparation of the final CD samples, aliquots of the oxidized and reduced hLF peptide solutions were added to aliquots of the respective buffers, micellar solutions, or lipid dispersions. The final peptide concentration in all samples was 17.5 μM, the SDS and DPC concentration in the micellar solutions was 10 mM (peptide-to-detergent ratio 1:570), and the lipid concentration in the vesicle dispersions was 1.45 mM (peptide-to-lipid ratio 1:80).

CD and UV Spectroscopy—CD spectra of the reduced and oxidized hLF peptide in phosphate buffer, in membrane-mimicking environments such as 50% trifluoroethanol, 50% phosphate buffer solution or SDS and DPC micellar solution, and in DMPC and DMPG/DMPC vesicle dispersions were recorded on a J-815 spectropolarimeter (Jasco, Gross-Umstadt, Germany) equipped with 1 mm-Suprasil quartz glass cells (Hellma, Müllheim, Germany). The samples were measured at a scan rate of 10 nm $\times$ min^{-1} and a 1-nm bandwidth in 0.1-nm intervals between 260 and 185 nm at 20 °C for the buffer and micellar solutions and at 30 °C for the vesicle suspensions, *i.e.* above the phase transition temperature of the lipids contained in the vesicle suspensions. Three repeat scans were averaged for each sample. CD spectra were smoothened by the adaptive smoothing of Jasco Spectra Analysis software, and the secondary structure was analyzed by the CONTINLL program with the implemented ridge regression algorithm (22, 23) provided on the DICHROWEB server (24, 25). The quality of the fit between experimental and back-calculated spectrum corresponding to the derived secondary structure element fractions was assessed from the normalized root mean square deviation with a value of <0.1 considered a good fit (25). For calculation of the mean

residue ellipticities used for the secondary structure estimation, the results were normalized to UV absorbance at 280 nm assuming a molar extinction coefficient of 5625 liters $\times$ mol^{-1} $\times$ cm^{-1} for the peptide with oxidized Cys residues and 5500 liters $\times$ mol^{-1} $\times$ cm^{-1} for reduced Cys residues (26). The absorption spectrum in the range of the aromatic bands due to tryptophan (and cystine for the oxidized peptide) was recorded in the range of 240 to 340 nm using a quartz glass half-micro-cuvette with 1-cm optical path length (Hellma). For correction of scattering, the base line of a log absorbance against log wavelength from the nonabsorbing region between 310 and 340 nm was extrapolated toward lower wavelengths and subtracted from the measured spectrum to get the final spectrum (27).

NMR—All NMR samples were prepared using a Shigemi NMR tube dissolving 0.83 mg of hLF in 300 μl of 95:5 (v:v) H$_2$O buffer/D$_2$O. Two-dimensional ROESY and NOESY experiments employing a WATERGATE solvent suppression scheme were performed at 10 or 20 °C on a Varian Inova 600-MHz spectrometer equipped with a 5-mm triple resonance three-axis gradient probe using a 200 ms ROE or NOE mixing period. The spectra were recorded as 2048 $\times$ 512 hypercomplex points with 9009.1 $\times$ 8000 Hz spectral widths for the F2 and F1 dimensions, respectively. Spectra were transformed using the nmrPipe processing package.

Surface Plasmon Resonance Binding Experiments—Surface plasmon resonance experiments were conducted as described previously (28). The reducing ends of 6-kDa HS were biotinylated by preactivated biotin-LC-hydrazide (Pierce). The biotinylation procedure was verified by streptavidin-peroxidase labeling after blotting of the material onto a ZetaProbe membrane. CM4 flow cell Biacore sensorchips were activated with 50 μl of 0.2 M N-ethyl-N'-(diethylaminopropyl)-carbodiimide and 0.05 M N-hydroxysuccinimide before injection of 50 μl of streptavidin (0.2 mg/ml in 10 mM acetate buffer, pH 4.2). The remaining activated groups were blocked with 50 μl of 1 M ethanolamine, pH 8.5. Typically, this procedure permitted the coupling of ~3.000–3.500 resonance units of streptavidin. Subsequently, the biotinylated HS (10 μg/ml) molecules were immobilized by injection over a one-surface flow cell leading to an immobilization level of ~50 resonance units. The flow cells were then conditioned with several injections of 2 M NaCl. Untreated one-flow cells served as the negative control. Binding assays were conducted with different concentrations of oxidized and reduced hLF in HBS-P at 25 °C and a flow rate of 20 μl/min. Regeneration of the sensorchip surface was achieved by a 5-min pulse of 2 M NaCl in HBS-P buffer.

RESULTS

Cellular Uptake of the Human Lactoferrin-derived Peptide— There are grave concerns about the potential immunogenicity of peptides used in biomedicine. This is especially the case when peptides are conjugated to larger molecular weight proteins. Given recent observations that certain antimicrobial peptides may act as cell-penetrating peptides, we selected a peptide corresponding to amino acids 38–59 of human lactoferrin as a potential candidate for a new CPP derived from a human protein. Previously, this peptide was shown to possess antimicrobial activity (29). The peptide comprises an exposed loop of the
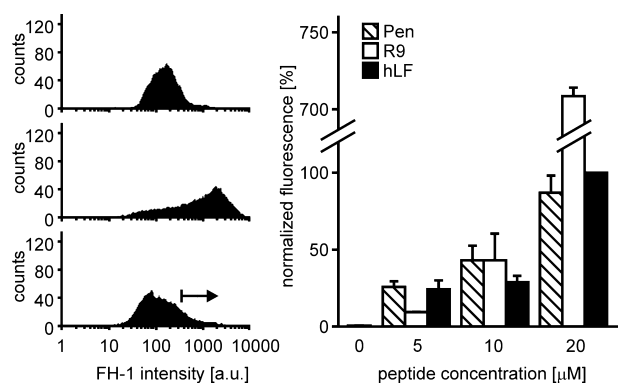
FIGURE 1. **Concentration dependence of uptake.** HeLa cells were incubated with increasing concentrations of the indicated peptides for 45 min. Afterward the cells were washed with cold PBS and harvested with trypsin/EDTA. Uptake into cells was analyzed by flow cytometry. *Left*, flow cytometry histograms of cells incubated with 20 μM solutions of penetratin (*top*), nona-arginine (R9) (*middle*), and hLF (*bottom*). The *arrow* in the *bottom panel* indicates the fraction of cells showing efficient peptide uptake. *Right*, median cellular fluorescence. The results of two independent experiments were normalized to median fluorescence for 20 μM hLF. The *error bars* correspond to the average deviation of two independent experiments. *Pen*, penetratin.

FIGURE 2. **Concentration-dependent phenotypes for the cellular uptake of the hLF peptide and toxicity.** *A*, HeLa cells were incubated for 30 min with different concentrations of the peptide. After two washing steps, the cellular peptide uptake was analyzed by confocal laser scanning microscopy. The *scale bar* indicates 20 μm. *B*, HeLa cells were incubated with increasing concentrations of the hLF peptide for 6 h (*squares*) or 24 h (*circles*), and subsequently cell viability was determined using the MTT assay.

lactoferrin protein that is terminally flanked by cysteine residues. These cysteine residues form a disulfide bridge, both in the protein and in lactoferricin, a naturally occurring degradation product of lactoferrin. In our peptide, at the N-terminal side of the first cysteine residue, a lysine residue of the lactoferrin sequence was preserved. Similarly, a lysine and an arginine residue from the lactoferrin sequence were included at the C terminus of the second cysteine residue. Given the requirement for positive charge to promote cellular uptake, we reasoned that these three residues should promote the function of the peptide as a CPP.

The peptide was synthesized as a peptide amide labeled with carboxyfluorescein at its N terminus. To apply stringent criteria for classifying this peptide as a potential new CPP, uptake was compared with the uptake of fluorescein-labeled analogs of the well established CPPs penetratin and R9. HeLa cells were incubated with these peptides at concentrations ranging from 5 to 20 μM, and uptake was quantified in living cells by flow cytometry. Trypsinization of cells (required to detach the cells from the tissue culture plate prior to flow cytometry) was used to remove peptides that were merely adsorbed to the outer plasma membrane.

All three peptides were taken up in a concentration-dependent manner, and no saturation of uptake was observed (Fig. 1). For penetratin, the cellular import was proportional to the concentration of peptide present in the medium. R9 uptake increased strongly at 20 μM, which very likely reflects the efficient cytoplasmic uptake via localized areas of the plasma membrane that we have called nucleation zones (NZ) (18). Uptake of the hLF peptide also showed clear concentration dependence. The relative increase in uptake from 10 to 20 μM was notably stronger than from 5 to 10 μM.

Intracellular Distribution of the hLF Peptide—Given our recent observation of a rapid cytoplasmic delivery of certain CPPs at higher concentrations, we were particularly interested in investigating the concentration dependence of the intracellular distribution of the hLF peptide. The intracellular localiza-
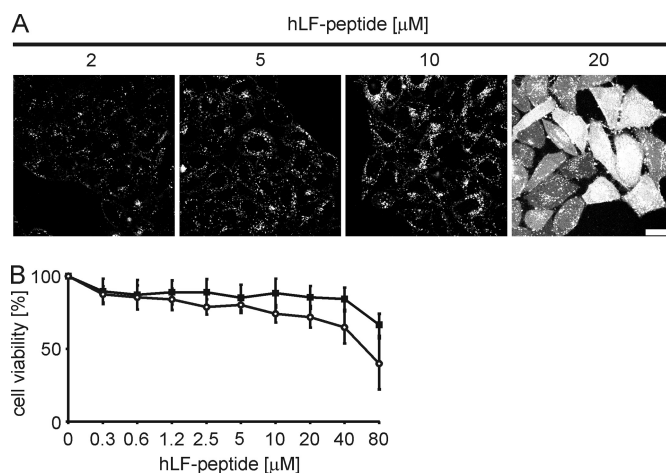
tion of the peptide in living cells was investigated by confocal microscopy. For concentrations up to 10 μM the peptide was localized predominantly in vesicles (Fig. 2*A*). In contrast, at a concentration of 20 μM, next to a vesicular staining, nearly all cells showed a homogeneous cytoplasmic and nuclear peptide distribution. This concentration dependence of the intracellular distribution very much resembled our former observations for the R9 and Tat peptides (18) of a cytoplasmic entry via NZ. In order to further establish that entry of the hLF peptide occurred via the same process, we followed the uptake by time lapse confocal fluorescence microscopy. This experiment confirmed the induction of NZ as the basis for rapid entry (not shown). We had shown previously that for arginine-rich peptides this rapid entry is associated neither with membrane damage nor with cytotoxicity. To exclude also for the hLF peptide the suggestion that cytoplasmic delivery results in cell death, HeLa cells were incubated with peptide for 6 and 24 h, and cell viability was assessed by the MTT assay. After 6 h of incubation the cells were viable at peptide concentrations up to 40 μM, whereas viability was reduced by 25% for cells incubated for 24 h at a peptide concentration of 10 μM.

Structure-Activity Relationship of the hLF Peptide for Efficient Uptake—After testing the uptake properties and intracellular distribution, we were interested in defining the structure-activity relationship of the hLF peptide for efficient cellular uptake. With 22 amino acids, the hLF peptide is a CPP of intermediate length. Four of the seven cationic amino acids and the aromatic amino acids are localized in the sequence nested between the cysteine residues. Positively charged and aromatic residues are typically associated with CPP activity. In the full-length protein, the cysteine residues form a disulfide bridge that constrains the domain into a loop conformation (30).

First, we wondered whether a shorter peptide would also show efficient import (Table 1). Removal of the three C-terminal residues following the cysteine residue was tolerated (Fig. 3*A*). In contrast, as soon as a cysteine residue was omitted,

TABLE 1

Primary structures of the peptides used in this study

All peptides were synthesized as C-terminal peptide amides (-CONH$_2$), rLF, rat lactoferrin; Fluo, 5(6)-carboxyfluorescein; Ahx, aminohexanoic acid.

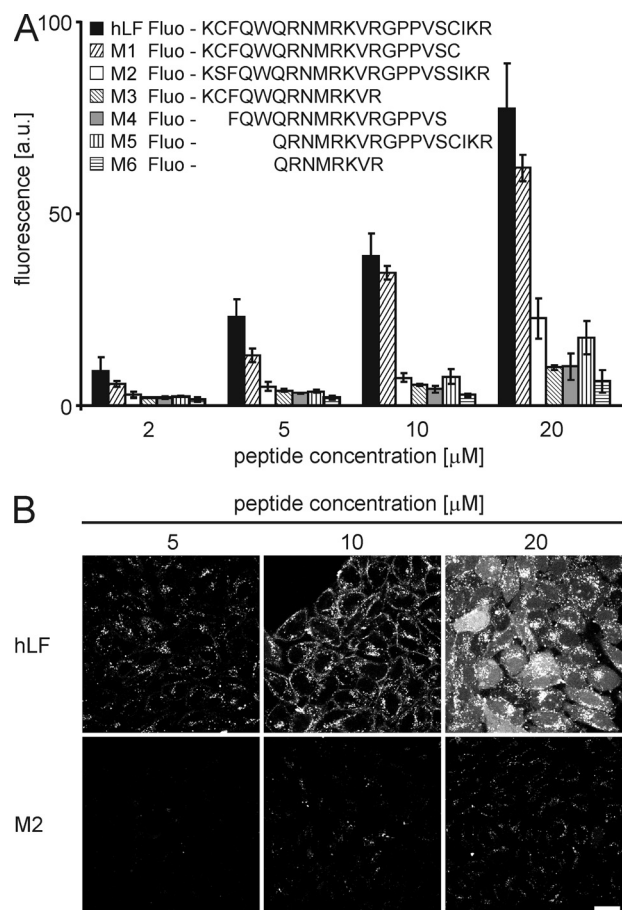| Peptide	Sequence
R9	Fluo-RRRRRRRRR-CONH$_2$
penetratin	Fluo-RQIKIWFQNRRMKWKK-CONH$_2$
rLF peptide	Fluo-KCFMWQEMLNKAGVPKLRCARK-CONH$_2$
hLF peptide	Fluo-KCFQWQRNMRKVRGPPVSCIKR-CONH$_2$
M1	Fluo-KCFQWQRNMRKVRGPPVSC-CONH$_2$
M2	Fluo-KSFQWQRNMRKVRGPPVSSIKR-CONH$_2$
M3	Fluo-KCFQWQRNMRKVR-CONH$_2$
M4	Fluo-FQWQRNMRKVRGPPVS-CONH$_2$
M5	Fluo-QRNMRKVRGPPVSCIKR-CONH$_2$
M6	Fluo-QRNMRKVR-CONH$_2$
Biotinylated hLF peptide	Biotin-Ahx-KCFQWQRNMRKVRGPPVSCIKR-CONH$_2$

FIGURE 3. **Structure-activity relationship of hLF.** *A*, HeLa cells were incubated with increasing concentrations of the indicated peptides for 30 min. Afterward the cells were washed and harvested with trypsin/EDTA. Uptake into cells was quantitated by flow cytometry. *B*, HeLa cells were incubated with increasing concentrations of the indicated peptides for 30 min, washed, and analyzed by confocal laser scanning microscopy. The *scale bars* indicate 20 μm. *a.u.*, arbitrary units.

import efficiency was reduced dramatically. This result suggested a structural requirement for the formation of the disulfide bridge in order to obtain efficient import. We therefore also tested a peptide in which the cysteine residues were exchanged for serine residues. Again, import of the resulting analog was reduced drastically. This finding further demonstrates that effi-

cient uptake can be attributed to the capacity of the cysteines to form a disulfide bridge. Formation of the disulfide bridge was confirmed analytically by mass spectrometry (see below). We validated the result by confocal microscopy, comparing the uptake of hLF and the Cys →Ser hLF mutant (M2) (Fig. 3*B*). For the mutant peptide the intracellular distribution was strictly vesicular. Also, at higher concentrations the cytoplasmic import could not be observed, demonstrating that this import was a function of the disulfide bridge.

Comparison with an hLF Analog of a Different Species—To test whether only the number of positively charged side chains was essential for efficient uptake or whether additional sequence-specific elements were also involved, the uptake of hLF was compared with a rat-derived lactoferrin peptide containing six positively charged amino acids *versus* seven for the hLF peptide. Especially for the sequence nested within the disulfide bridge, the position of positively charged residues differed. Neither for HeLa cells nor for rat IEC-6 cells was an efficient cytoplasmic uptake observed (Fig. 4), indicating the importance of the specific sequence of hLF and that efficient uptake is not related to the species from which the peptide and target cells originated.

Structural Analyses—The cellular uptake experiments provided strong functional evidence for the requirement of cyclization for the efficient cellular import of the hLF peptide. Therefore, we next addressed explicitly the structure of the peptide and how this structure depends on the presence of the disulfide bridge. The hLF peptide comprises the loop and one disulfide bridge of human lactoferricin, which at pH 4 forms a nascent helix (31). Formation of the disulfide bridge upon oxidation was confirmed by mass spectrometry (Fig. 5, *A* and *B*).

First, we addressed conformational differences in the reduced and oxidized cyclic form of the peptide using NMR. The spectra showed relatively broad and ill-defined peaks and only limited ROE cross-peak patterns. In particular, no amide-amide ROE or NOE cross-peaks indicative of helix formation were observed, and amide-H$^\alpha$ cross-peaks in the fingerprint region did not identify significantly downfield-shifted H$^\alpha$ resonances indicative of extended conformation and expected for the N-terminal residues of the peptide (Fig. 5*C*). The absence or presence of the disulfide bridge did not result in major changes in the appearance of the NMR spectra. Lowering the temperature to 10 °C also did not result in a substantial improvement of the spectrum. In contrast to the NOE spectra recorded previously for the longer lactoferricin peptide (13), the ROESY spectra recorded on the hLF discriminated cross-peaks resulting from the ROE from those originating from chemical exchange on the basis of their sign. Interestingly, clear exchange cross-peaks were observed in the aromatic/amide region as well as in the aliphatic region of the spectrum (Fig. 5, *D* and *E*). Dissolving the peptide in the solvent mixture H$_2$O:CD$_3$OD:CDCl$_3$ (1:4:4 (w/w/w)) as done previously (31) did not radically change the spectral appearance, although an increase in spectral dispersion was observed, and weak, upfield-shifted H$^\alpha$ resonances as well as downfield-shifted methyl resonances suggested the formation of an extended structure (not shown). However, relatively broad lines were again observed in conjunction with a lack of cross-peaks in the fingerprint and amide regions. It is notewor-
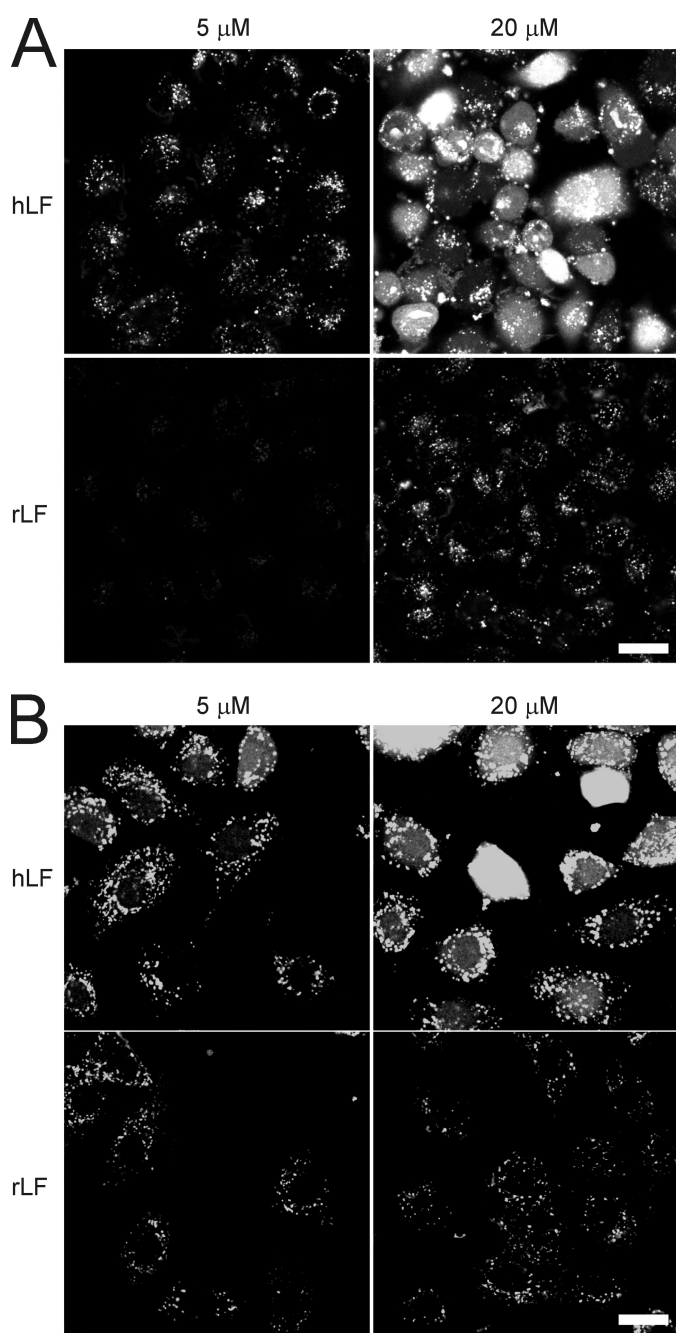
FIGURE 4. Comparison of the uptake of human (*hLF*) and rat-derived LF (*rLF*) peptides in HeLa (*A*) and rat IEC-6 (*B*) cells. Cells were incubated with 5 and 20 μM human or rat lactoferrin for 60 min at 37 °C in RPMI supplemented with 10% fetal calf serum. Cells were washed twice and imaged immediately using confocal microscopy. The *scale bars* indicate 20 μm.

FIGURE 5. **Structural analyses at micellar membranes.** *A* and *B*, electron spray mass spectrometry of the reduced (*A*) and oxidized (*B*) forms of the hLF peptide. The signals of the differently charged species of the molecules correspond to an *m/z* difference of +2 Da of the reduced form of the peptide. *C*, NOESY spectrum of 1 mM hLF in H_2O solution. *D* and *E*, upfield (*D*) and aliphatic (*E*) regions of the ROESY spectrum of hLF in H_2O solution. Cross-peaks with negative intensity (corresponding to ROE peaks) are shown as single contours, whereas cross-peaks with positive signs (corresponding to the diagonal and exchange peaks) are shown with multiple, exponentially spaced contours. *F* and *G*, CD spectroscopy in an aqueous phosphate buffer (*F*) and phosphate buffer containing DMPC/DMPG 3:1 vesicles (*G*). *H* and *I*, data analysis via the CONTINLL algorithm of the reduced peptide (*H*) and the oxidized hLF peptide (*I*). Especially at the surface of DMPC/DMPG 3:1 vesicles (indicated by *arrows*), β-strand formation was induced for the oxidized form of the peptide.

thy that under all conditions, the single, easily identifiable Trp[42] (Trp[5] peptide) side chain N1 proton shows as much as four different resonances of varying intensities. Overall, the NMR data suggest a potentially oligomeric, partially folded state, subject to conformational exchange.

Having failed to observe an oxidation-dependent conformational difference in an aqueous buffer, we next employed CD spectroscopy to obtain information about the secondary structure in membrane-mimicking environments and in buffers containing micelles or vesicles. Consistent with the NMR anal-
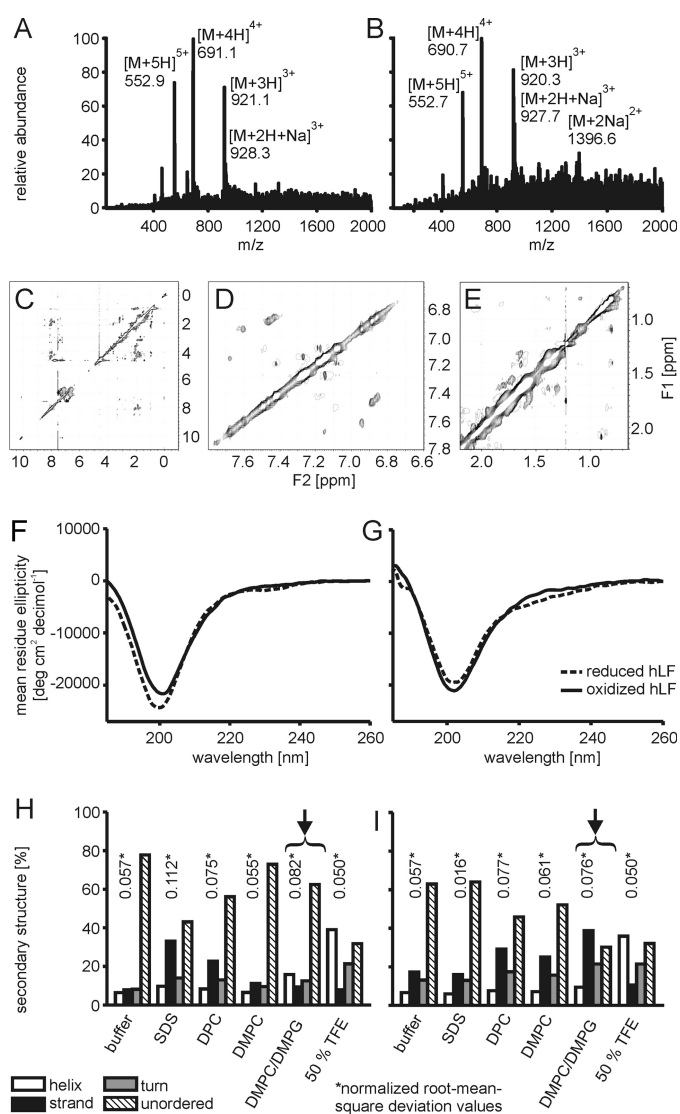
ysis, in aqueous buffer, reduction of the disulfide bridge by incubation with dithiothreitol had no effect on the shape of the CD spectrum in a temperature range of 5 to 20 °C (not shown). The CD spectra could not be described by a linear combination of CD spectra for classical secondary structure elements, *i.e.* α-helix, β-sheet, and random coil. However, the spectrum was also distinct from that expected for purely random coil. The addition of 50% trifluoroethanol led to the formation of an α-helix in the reduced and oxidized states of the peptide.

In contrast, both forms showed different spectra in solutions containing detergent or lipid. SDS increased the β-sheet con-

tent in the reduced form only, whereas DPC increased the content in the reduced and in the oxidized form. In contrast, for DMPC and DMPC/DMPG, the β-sheet content increased only for the oxidized form, with DMPC/DMPG inducing the most pronounced changes (Fig. 5, *F--I*). The latter results demonstrate that oxidation affects the capacity of the peptide to undergo conformational changes.

Binding of the hLF Peptide and hLF Cys $\rightarrow$ Ser to Heparan Sulfate Proteoglycans—Heparan sulfate proteoglycans reportedly contribute to the uptake of several CPPs (32, 33). Therefore, these sugars may also contribute to the dependence of uptake on the presence of the disulfide bridge. We addressed the binding of the oxidized and reduced hLF peptide to HS chains with an SPR-based binding assay, a physiologically relevant system in which a low amount of HS is coupled through its reducing end to a sensorchip, thus representing HS proteoglycan presentation at the cell surface. Injection of reduced hLF over this surface, in the 250 to 3000 nM range, gave binding curves that reached a plateau at 25–75 resonance units, whereas the oxidized form of the peptide gave binding curves reaching a plateau at 48–156 resonance units (Fig. 6). From the binding curves of the oxidized peptide, a K_D value of 2 μM was obtained. In a similar set of experiments in which binding of fluorescein-labeled hLF was compared with binding of the flu-

orescein-labeled Cys $\rightarrow$ Ser mutant, a K_D value of 10 μM was obtained for the wild-type hLF, whereas no binding could be detected for the mutant peptide (not shown). These results validate the specificity of binding of the hLF peptide for HS. The residual binding obtained for the reduced peptide may be due to incomplete reduction.

HS Proteoglycan Dependence and Rottlerin Sensitivity of the Uptake—Having observed a strong conformational dependence of the binding of the hLF peptide to HS using biochemical assays, we next addressed the relevance of this interaction for the binding to cells. Removal of HS chains after a 1-h treatment with heparinases I–III nearly abolished the binding of the hLF peptide to the cell surface and reduced the number and intensity of vesicles (Fig. 7*A*).

Furthermore, we tested the effect of rottlerin on the cytoplasmic uptake of the oxidized hLF peptide. Rottlerin was described originally as a PKC inhibitor with its strongest activity toward the protein kinase C-δ isoform (35). However, the specificity was questioned later (36). Previously, we showed that this drug acts as an effective inhibitor of cellular peptide uptake via nucleation zones (18). Cells were preincubated with rottlerin, and peptide uptake was analyzed by flow cytometry and fluorescence microscopy (Fig. 7, *B* and *C*). At low peptide concentrations, at which only vesicular uptake occurred, rottlerin reduced uptake only weakly. At peptide concentrations at which uptake via NZ occurred, peptide uptake was inhibited by up to 50%. Confocal microscopy confirmed that rottlerin only inhibits efficient cytoplasmic peptide uptake. The concentration-dependent increase in cell-associated fluorescence observed in the presence of rottlerin (Fig. 7*B*) may therefore be attributed to vesicular peptide uptake, which is not affected by rottlerin.

hLF-mediated Import of Protein Cargos—The ability to mediate the cellular uptake of a diverse set of cargos is an important characteristic for a CPP, making it valuable for applications in biological and biomedical research. As such, the fluorophore could already be considered a cargo, as it may affect the cellular trafficking of a CPP (37). Therefore, our data suggest that lactoferrin is well suited for the efficient cellular import of small molecules that otherwise cross the plasma membrane only poorly.

In addition, we tested whether the hLF peptide was able to mediate the import of a large molecular weight protein cargo. For these complexes, potential immunogenicity of the CPP is an important concern. Therefore, using a human protein-derived peptide is of particular importance. To this end, a biotinylated hLF was synthesized and coupled to Alexa 488-labeled streptavidin in a molar ratio of 4:1 (peptide:streptavidin). Import of these conjugates into HeLa cells was
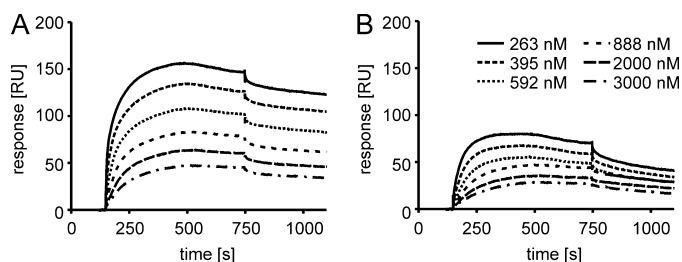

FIGURE 6. **Affinity measurements of oxidized (*A*) and reduced (*B*) hLF for HS-coated surfaces using SPR.** *RU*, resonance units.
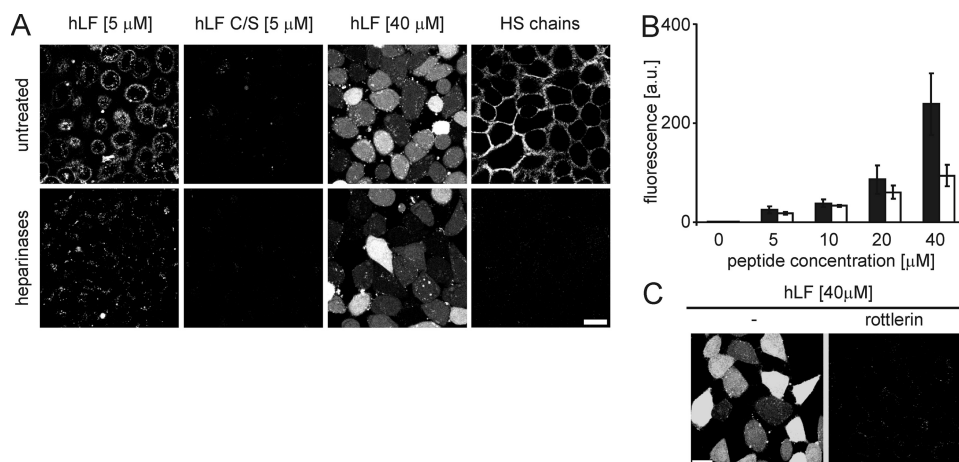

FIGURE 7. **Cytoplasmic import of hLF is HS proteoglycan-dependent and negatively affected by rottlerin.** *A*, HeLa cells were treated for 1 h with heparinases I, II, and III (33, 8, and 5 mIU/ml, respectively) or remained untreated. Subsequently, the cells were washed and incubated with different concentrations of the hLF peptide. Images were taken after 30 min of peptide incubation. Removal of HS chains from the cell surface was confirmed by immunofluorescence staining of treated and untreated cells. *B* and *C*, HeLa cells were treated with 20 μM rottlerin for 30 min or remained untreated. After one washing step the cells were incubated with different concentrations of hLF in the presence (*white bars*) or absence of rottlerin (*black bars*) (*B*). After 30 min of incubation the cells were analyzed by flow cytometry or confocal laser scanning microscopy (*C*). The *scale bars* indicate 20 μm. *a.u.*, arbitrary units.

StavAlexa488 +

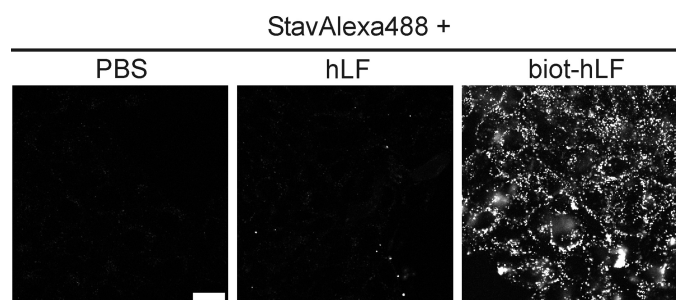| PBS	hLF	biot-hLF

FIGURE 8. **Biotinylated hLF peptide efficiently transports streptavidin-Alexa 488 into cells.** HeLa cells were incubated for 30 min with biotinylated hLF-streptavidin-Alexa 488 complex (5 μM). After two washing steps, cellular uptake was analyzed by confocal laser scanning microscopy. Coincubations of streptavidin with PBS (*left*) and non-biotinylated hLF peptide (*middle*) served as controls. The *scale bar* indicates 20 μm.

visualized by confocal fluorescence microscopy (Fig. 8). Streptavidin-Alexa 488 was internalized into vesicular compartments in accordance with observations for high molecular weight complexes of other CPPs (20). This uptake occurred only when the protein was conjugated to biotinylated hLF peptide. Neither the protein alone nor the protein in the presence of non-biotinylated hLF peptide was taken up.

DISCUSSION

The results shown in this article present a new cell-penetrating peptide corresponding to amino acids 38–59 of human lactoferrin (amino acids 19–40 of human lactoferricin). With 22 amino acids, the hLF peptide is a CPP of intermediate length. Nevertheless, repeated batches of the peptide obtained by solid-phase peptide synthesis following standard procedures showed the typical purities of the N-terminally labeled peptide to be about 80%.

In contrast to shorter ones, oligoarginine peptides of more than eight amino acids in length enter cells more efficiently and show a concentration-dependent uptake mechanism into the cytoplasm (19). Even though the hLF peptide contains less arginine residues than the Tat peptide or R9, a concentration-dependent uptake mechanism was also observed. At concentrations higher than 10 μM, the peptide rapidly enters the cytoplasm. The sensitivity of this uptake to rottlerin treatment of cells suggests that this mechanism is the same as observed for R9 and the Tat peptide. Thus far, the rottlerin-sensitive uptake mechanism had been observed only for arginine-rich CPPs. Our observations on the conformation-dependent uptake of the hLF peptide suggest that the particular structure of this peptide may functionally replace the high arginine content for this mechanism of cell entry.

The sequence nested within the two cysteine residues is reminiscent of cationic amphipathic CPPs such as penetratin. However, removal of the disulfide bridge, either by reduction of cysteine residues (not shown) or their replacement by serine residues, strongly reduced the capacity of the peptide to enter cells. To our knowledge, this is the first report of a cell-penetrating peptide that requires a cyclic structure for its activity. However, numerous antimicrobial peptides have been investigated to this aim, such as gramicidin S (38), protegrin-1 (39), RTD-1 (40), ranatuerin-1 (41), bactenecin (42), and tachyplesin-1 (43–45), although with differing results. In the latter case,

aggregation was found to be the deactivating factor, which could be prevented by proper cyclization.

Dependence on a disulfide bridge for efficient import is not predicted by our current knowledge of CPPs. A prediction identified the central QWQRNMRKVR motif as essential for CPP activity (46). The terminal residues in the cysteine-containing wild-type peptide as well as the serine-containing mutant analog are not predicted to influence the uptake significantly.[6] Furthermore, comparison with the corresponding disulfide bridge-containing rat-derived lactoferrin peptide identified the hLF peptide as a far superior CPP, despite a similar number of positively charged amino acids. These considerations indicate that for the hLF peptide, a simple examination of the primary structure fails to predict the structural determinants required for efficient cell entry of the peptide. The hLF also demonstrated a more efficient uptake compared with rat lactoferrin in IEC-6 rat cells, indicating the absence of an evolutionary constraint on the internalization efficiency.

In the crystal structure of human lactoferrin (47), the residues corresponding to hLF are part of an α-β-α motif that is stabilized by the formation of a disulfide bridge between Cys[39] and Cys[56] (positions 2 and 19 in the peptide) and hydrophobic interactions that involve Trp[42] and Val[54] (positions 5 and 17 in the peptide) and Met[46] and Pro[52] (positions 9 and 15 in the peptide). For the human lactoferricin peptide, NMR data indicate that the amino acid residues corresponding to the hLF peptide adopt a "nascent" helical structure in aqueous solutions and a conformation resembling the crystal structure in membrane-mimicking solvent. Our data clearly show the necessity of the presence of the Cys[39]-Cys[56] (positions 2 and 19 in the peptide) disulfide bridge for efficient import. However, in solution, neither CD nor NMR spectra were significantly affected by disulfide formation. Whereas the CD data indicate a non-random coil conformation of hLF, the NMR data also point to conformational exchange. It is tempting to speculate that Trp[42] (position 5 in the peptide) is a crucial factor affecting the NMR spectra because of its essential structural role and the putative large changes in shielding effects that it exerts. Other dynamic effects, such as dimer formation, could similarly affect the NMR spectra; such a phenomenon was postulated for the longer human lactoferricin peptide in aqueous solvent (31).

Therefore, CD spectra were also recorded in the presence of phospholipid micelles in order to gain further insights into the structural impact of lipid surfaces on the peptide. Here, the oxidized peptide showed a clear preference for β-strand formation, whereas the reduced peptide presented no defined secondary structure. Interestingly, the differences in secondary structure formation between the oxidized and reduced hLF peptide were most pronounced in the presence of DMPC/DMPG vesicles; this ensures strong electrostatic attraction of the peptide and is also a good mimic of the cellular membrane environment. Additionally, the interaction with heparan sulfate chains was investigated by surface plasmon resonance and in cellular assays. SPR experiments showed that the interaction with HS is enhanced significantly upon oxidation of the peptide.

---

[6] M. Hällbrink, personal communication.

Cellular assays show the physiological relevance of the different HS-peptide interactions. In cell experiments we made an interesting additional observation concerning the involvement of HS proteoglycans in NZ-dependent cytoplasmic uptake. Consistent with our previous results, heparinase treatment over a period of 6 h abolished the rapid cytoplasmic uptake of hLF (not shown). In contrast, short term treatment over only 1 h had no significant effect on NZ-dependent import. However, membrane binding of hLF at lower peptide concentrations was strongly reduced. We therefore concluded that the previously observed effect of long term heparinase treatment on NZ-dependent uptake was due to perturbations of membrane protein organization or molecular events involved in this cytoplasmic uptake.

Given that the cell uptake experiments did not show any concentration-dependent saturation, the lactoferrin-derived CPP exhibited one of the most prominent characteristics for the uptake of CPPs. In the full-length lactoferrin protein, cellular uptake has been described for various cellular systems. Although it has been observed that the polycationic nature of the N terminus by itself confers an interaction with sugars on the cell surface, cellular uptake and the biological effects of lactoferrin have been attributed to its binding to one of the several receptors identified for this protein (48). In contrast to our peptide, binding to these receptors was therefore saturable. Quite remarkably, regarding binding to the lymphocyte lactoferrin receptor and the platelet lactoferrin receptor, evidence has been obtained for the involvement of the loop domain corresponding to the lactoferrin-derived CPP (49, 50). Competition experiments with our peptide for the binding of lactoferrin may thus help to better define ligand binding domains for other types of lactoferrin receptors.

In summary, the results show that the hLF peptide is a new CPP with highly interesting structural and functional characteristics. With respect to the mechanism of import, we expect that further analyses of the structure-activity relationship will yield new insights into the molecular determinants of the cell surface that mediate the molecular interaction and induce the efficient cellular import via nucleation zones. Furthermore, it will be interesting to compare analogous peptides derived from lactoferrin of different species. In the past, the antimicrobial characteristics of bovine lactoferrin-derived peptides have been compared in detail with those of their human counterparts (13). Because of its human origin, the hLF peptide is expected to be non-immunogenic. For this reason, this molecule is a candidate vector for biomedical applications, especially for the import of high molecular weight complexes.

REFERENCES

1. Derossi, D., Joliot, A. H., Chassaing, G., and Prochiantz, A. (1994) *J. Biol. Chem.* **269,** 10444–10450
2. Vivès, E., Brodin, P., and Lebleu, B. (1997) *J. Biol. Chem.* **272,** 16010–16017
3. Fischer, P. M., Krausz, E., and Lane, D. P. (2001) *Bioconjug. Chem.* **12,** 825–841
4. Järver, P., Langel, K., El-Andaloussi, S., and Langel, U. (2007) *Biochem. Soc. Trans.* **35,** 770–774
5. Foerg, C., and Merkle, H. P. (2008) *J. Pharm. Sci.* **97,** 144–162
6. Ding, G. J., Fischer, P. A., Boltz, R. C., Schmidt, J. A., Colaianne, J. J., Gough, A., Rubin, R. A., and Miller, D. K. (1998) *J. Biol. Chem.* **273,** 28897–28905
7. Rojas, M., Donahue, J. P., Tan, Z., and Lin, Y. Z. (1998) *Nat. Biotechnol.* **16,** 370–375
8. Metz-Boutigue, M. H., Jollès, J., Mazurier, J., Schoentgen, F., Legrand, D., Spik, G., Montreuil, J., and Jollès, P. (1984) *Eur. J. Biochem.* **145,** 659–676
9. Levay, P. F., and Viljoen, M. (1995) *Haematologica* **80,** 252–267
10. Legrand, D., Pierce, A., Elass, E., Carpentier, M., Mariller, C., and Mazurier, J. (2008) *Adv. Exp. Med. Biol.* **606,** 163–194
11. Ward, P. P., and Conneely, O. M. (2004) *Biometals* **17,** 203–208
12. Valenti, P., and Antonini, G. (2005) *Cell. Mol. Life Sci.* **62,** 2576–2587
13. Gifford, J. L., Hunter, H. N., and Vogel, H. J. (2005) *Cell. Mol. Life Sci.* **62,** 2588–2598
14. Bellamy, W., Takase, M., Yamauchi, K., Wakabayashi, H., Kawase, K., and Tomita, M. (1992) *Biochim. Biophys. Acta* **1121,** 130–136
15. Takeshima, K., Chikushi, A., Lee, K. K., Yonehara, S., and Matsuzaki, K. (2003) *J. Biol. Chem.* **278,** 1310–1315
16. Nekhotiaeva, N., Elmquist, A., Rajarao, G. K., Hällbrink, M., Langel, U., and Good, L. (2004) *FASEB J.* **18,** 394–396
17. Elass-Rochard, E., Roseanu, A., Legrand, D., Trif, M., Salmon, V., Motas, C., Montreuil, J., and Spik, G. (1995) *Biochem. J.* **312,** 839–845
18. Duchardt, F., Fotin-Mleczek, M., Schwarz, H., Fischer, R., and Brock, R. (2007) *Traffic* **8,** 848–866
19. Kosuge, M., Takeuchi, T., Nakase, I., Jones, A. T., and Futaki, S. (2008) *Bioconjug. Chem.* **19,** 656–664
20. Tünnemann, G., Martin, R. M., Haupt, S., Patsch, C., Edenhofer, F., and Cardoso, M. C. (2006) *FASEB J.* **20,** 1775–1784
21. van Kuppevelt, T. H., Dennissen, M. A., van Venrooij, W. J., Hoet, R. M., and Veerkamp, J. H. (1998) *J. Biol. Chem.* **273,** 12960–12966
22. Provencher, S. W., and Glöckner, J. (1981) *Biochemistry* **20,** 33–37
23. van Stokkum, I. H., Spoelder, H. J., Bloemendal, M., van Grondelle, R., and Groen, F. C. (1990) *Anal. Biochem.* **191,** 110–118
24. Lobley, A., Whitmore, L., and Wallace, B. A. (2002) *Bioinformatics* **18,** 211–212
25. Whitmore, L., and Wallace, B. A. (2004) *Nucleic. Acids Res.* **32,** W668–673
26. Pace, C. N., Vajdos, F., Fee, L., Grimsley, G., and Gray, T. (1995) *Protein Sci.* **4,** 2411–2423
27. Kelly, S. M., Jess, T. J., and Price, N. C. (2005) *Biochim. Biophys. Acta* **1751,** 119–139
28. Gidwani, P., Ramesh, K. H., Liu, Y., and Kolb, E. A. (2008) *Chemotherapy* **54,** 120–124
29. Groenink, J., Walgreen-Weterings, E., van't Hof, W., Veerman, E. C., and Nieuw Amerongen, A. V. (1999) *FEMS Microbiol. Lett.* **179,** 217–222
30. Peterson, N. A., Anderson, B. F., Jameson, G. B., Tweedie, J. W., and Baker, E. N. (2000) *Biochemistry* **39,** 6625–6633
31. Hunter, H. N., Demcoe, A. R., Jenssen, H., Gutteberg, T. J., and Vogel, H. J. (2005) *Antimicrob. Agents Chemother.* **49,** 3387–3395
32. Poon, G. M., and Gariepy, J. (2007) *Biochem. Soc. Trans.* **35,** 788–793
33. Tyagi, M., Rusnati, M., Presta, M., and Giacca, M. (2001) *J. Biol. Chem.* **276,** 3254–3261
34. Deleted in proof
35. Gschwendt, M., Müller, H. J., Kielbassa, K., Zang, R., Kittstein, W., Rincke, G., and Marks, F. (1994) *Biochem. Biophys. Res. Commun.* **199,** 93–98
36. Davies, S. P., Reddy, H., Caivano, M., and Cohen, P. (2000) *Biochem. J.* **351,** 95–105
37. Dupont, E., Prochiantz, A., and Joliot, A. (2007) *J. Biol. Chem.* **282,** 8994–9000
38. Wadhwani, P., Afonin, S., Ieronimo, M., Buerck, J., and Ulrich, A. S. (2006) *J. Org. Chem.* **71,** 55–61
39. Buffy, J. J., Waring, A. J., Lehrer, R. I., and Hong, M. (2003) *Biochemistry* **42,** 13725–13734
40. Selsted, M. E. (2004) *Curr. Protein Pept. Sci.* **5,** 365–371
41. Sonnevend, A., Knoop, F. C., Patel, M., Pál, T., Soto, A. M., and Conlon,

J. M. (2004) *Peptides* **25,** 29–36

42. Wu, M., and Hancock, R. E. (1999) *J. Biol. Chem.* **274,** 29–35
43. Matsuzaki, K., Yoneyama, S., Fujii, N., Miyajima, K., Yamada, K., Kirino, Y., and Anzai, K. (1997) *Biochemistry* **36,** 9799–9806
44. Ramamoorthy, A., Thennarasu, S., Tan, A., Gottipati, K., Sreekumar, S., Heyl, D. L., An, F. Y., and Shelburne, C. E. (2006) *Biochemistry* **45,** 6529–6540
45. Doherty, T., Waring, A. J., and Hong, M. (2008) *Biochemistry* **47,** 1105–1116
46. Hällbrink, M., Kilk, K., Elmquist, A., Lundberg, P., Lindgren, M., Jiang, Y.,

Pooga, M., Soomets, U., and Langel, Ü. (2005) *Int. J. Pept. Res. Ther.* **11,** 249–259
47. Sun X. L., Baker H. M., Shewry S. C., Jameson G. B., and Baker, E. N. (1999) *Acta Crystallogr. D Biol. Crystallogr.* **55,** 403–407
48. Suzuki, Y. A., Lopez, V., and Lönnerdal, B. (2005) *Cell. Mol. Life Sci.* **62,** 2560–2575
49. Legrand, D., Mazurier, J., Elass, A., Rochard, E., Vergoten, G., Maes, P., Montreuil, J., and Spik, G. (1992) *Biochemistry* **31,** 9243–9251
50. Leveugle, B., Mazurier, J., Legrand, D., Mazurier, C., Montreuil, J., and Spik, G. (1993) *Eur. J. Biochem.* **213,** 1205–1211